Intrinsic Impurity-Band Stoner Ferromagnetism in $C_{60}H_n$

Kyu Won Lee and Cheol Eui Lee*

Department of Physics and Institute for Nano Science, Korea University, Seoul 136-713, Korea

(Received 17 December 2010; published 20 April 2011)

We identify Stoner ferromagnetism in fcc $C_{60}H_n$ (n = odd) by using a local density approximation in the framework of the density functional theory. Hydrogen chemisorption on fullerenes creates quasilocalized π electrons on the fullerene surface, overlapping of their wave functions giving rise to a narrow half filled impurity band in the fcc $C_{60}H_n$. The Stoner-type ferromagnetic exchange between the itinerant electrons leads to spin-split impurity bands. The magnetic moment per $C_{60}H_n$ molecule is 1 μ_B (for n = odd) or 0 (for n = even, including zero), only one of the hydrogens contributing to the spin-split states. Direct overlapping of the quasilocalized π-electron orbitals is essential for the ferromagnetism.

DOI: 10.1103/PhysRevLett.106.166402 PACS numbers: 71.20.Tx, 71.70.Gm, 75.10.Lp, 75.50.Dd

Room-temperature ferromagnetism in polymerized rhombohedral fullerenes generated great interest as well as controversy on ferromagnetism in carbon [1–4]. Electronic structure calculations based on the density functional theory (DFT), incidentally, have revealed the absence of magnetic ordering in rhombohedral fullerene polymers [5,6]. Whether extrinsic iron impurities or intrinsic defects give rise to ferromagnetism is still a controversial issue [7–9]. Photo-oxidated fullerenes, on the other hand, have been shown to be ferromagnetic at room temperature [10–12].

Defects such as carbon vacancies in polymerized fullerenes and doped fullerenes $C_{60}R_n$ (R: nonmagnetic elements such as H and O) were considered as the origin of the intrinsic ferromagnetism in fullerenes. Carbon vacancies create magnetic moments in fullerenes but do not give rise to a ferromagnetic long-range order in polymerized fullerenes [13]. A recent DFT calculation on $C_{60}O$ revealed that oxygen promotes photopolymerization but does not create magnetic moments [14], an important role of hydrogen in ferromagnetism having been revealed [15–18].

In graphene, two types of hydrogen defects have been investigated in the framework of DFT, one of them being chemisorbed on carbon and the other being substituted for carbon vacancy bonding to one of the three neighboring carbons. The former leads to a Stoner type of ferromagnetic metal with a narrow spin-split impurity band [19], while the latter leads to a ferromagnetic insulator [20]. Polymerized fullerenes with hydrogen defects substituted for carbon vacancies are known as ferromagnetic insulators [21]. Dimerized fullerenes with chemisorbed hydrogen $(C_{60}H)_2$ have a triplet ground state [22]. Magnetic moments arise from the quasilocalized π electrons of carbons in the neighborhood of a hydrogenated carbon atom, a spin alternation model for the π-bonded carbon network having been adopted for the ferromagnetic long-range order [19–22].

The most stable form of fullerenes is a fcc crystal. While the fcc C_{60} is a van der Waals crystal, polymerized fullerenes are formed by covalent bonding with a much shorter interfullerene distance than that of fcc C_{60}. While the first well-established ferromagnetic fullerenes are monoclinic tetrakis(dimethylamino)ethylene-C_{60} crystals [23,24], room-temperature ferromagnetism taking place in fcc $C_{60}H_n$ crystals certainly deserves due attention [25,26]. In this work, we have investigated ferromagnetism in the fcc $C_{60}H_n$ crystals by performing a DFT calculation within the local density approximation (LDA), revealing the spin-split impurity band of Stoner type to be the origin of the ferromagnetism.

A SIESTA package [27] was employed for the DFT calculation within a LDA with an energy cutoff 200 Ry and k points of $4 \times 4 \times 4$ mesh in a Monkhorst-Pack scheme. The lattice parameters were taken for a fcc C_{60} crystal (a = 14.166 Å), and the atomic coordinates and geometry were optimized by using the conjugated gradients method, with a maximum force tolerance of 0.01 eV/Å for all the $C_{60}H_n$ molecules, crystals, and polymers investigated. The fcc $C_{60}H_n$ with a small n was assumed to have the same lattice parameters as those of the fcc C_{60} [25]. The calculated band structure of fcc C_{60} showed a direct band gap of ~1.06 eV at the X point in the fcc Brillouin zone [28].

Figures 1 and 2, respectively, show the electronic structure and the local density of states (LDOS) near the Fermi energy (E_F) of the $C_{60}H_n$ (n = 1–5) molecules. In the electronic structure of $C_{60}H_n$ with n odd, spin-split states near E_F give a magnetic moment of 1 μ_B per $C_{60}H_n$, while $C_{60}H_n$ with even n shows no spin-split states, with no magnetic moments [29]. Hydrogen chemisorption removes the degeneracy of the electronic states of C_{60}. While the electronic structure of $C_{60}H$ can be characterized by the spin-split states near E_F, that of $C_{60}H_2$ can be characterized by the highest-occupied molecular orbital. The electronic structure of $C_{60}H_3$ is quite close to a sum of those of $C_{60}H$ and $C_{60}H_2$, indicating that the electronic properties of $C_{60}H_n$ can be described by a superposition of one-hydrogen chemisorption and two-hydrogen chemisorption

 © 2011 American Physical Society

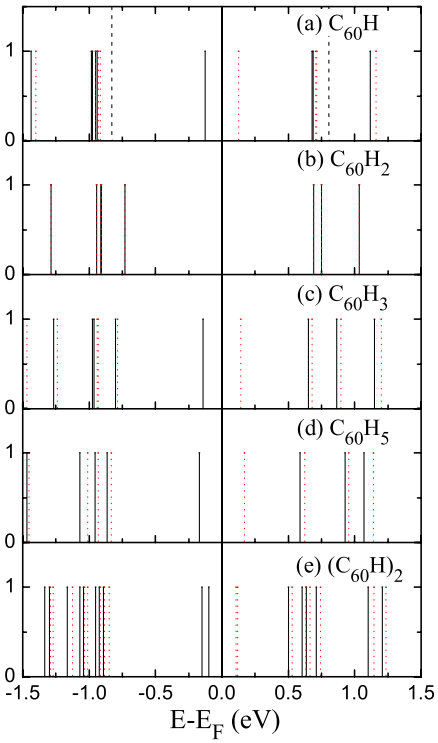

FIG. 1 (color online). Electronic structure of the $C_{60}H_n$ molecules. The dashed (black) line in (a) corresponds to C_{60}. The solid (black) and dotted (red) lines correspond to the spin-up and -down states, respectively.

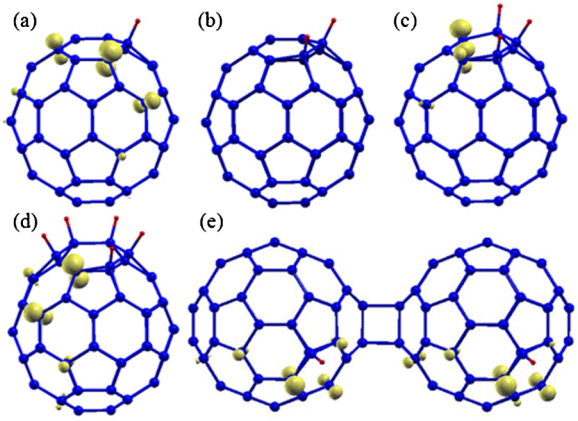

FIG. 2 (color online). Local density of states of the $C_{60}H_n$ molecules near the Fermi energy for (a) $n = 1$, (b) $n = 2$, (c) $n = 3$, (d) $n = 5$ and for (e) $(C_{60}H)_2$. The small (red) and medium-size (blue) circles correspond to hydrogen and carbon, respectively, the large (green) circles corresponding to the isosurface of the local density of states.

cases. A slight spin splitting in the valence states of $C_{60}H_n$ with n odd can be attributed to the exchange spin-polarization effect, the response of the fully populated valence states to the magnetization of the spin-split states resulting in a spin density of an opposite sign on the nearest-neighbor sites [19]. The LDOS of $C_{60}H_n$ with n odd shows that the electrons near E_F in the spin-split states are quasilocalized, i.e., delocalized over a fullerene surface centered at the carbon opposite to the hydrogen-chemisorbed one [21,22]. The LDOS near E_F is on the next-nearest-neighbor sites only, reflecting the underlying spin alternation mechanism.

Figure 3 shows the spin-degenerate and the spin-polarized band structures of fcc $C_{60}H$ with a total energy difference calculated to be 0.2 eV that can be taken as an effective exchange interaction energy. Chemisorbed hydrogen produces a narrow half filled impurity band within the band gap, and thus the fcc $C_{60}H$ is a narrow-band metal in the absence of exchange interaction [see Fig. 3(a)]. The chemisorbed hydrogen can be regarded as a donor providing a single state and a single electron leading to the half filled impurity band. The exchange interaction between the itinerant electrons in the impurity band renders the impurity band spin-split [see Fig. 3(b)]. The exchange splitting, i.e., the energy separation between the two spin-split bands, is also ~0.2 eV with only a slight fluctuation along the symmetry line of the Brillouin zone. The exchange interaction between the itinerant electrons thus gives rise to the spin-split bands, with the spin splitting occurring at E_F. It is compatible with the Stoner model for ferromagnetic metals, but spin splitting much greater than the impurity-band width of ~0.15 eV and the half filled impurity band lead to a ferromagnetic semiconductor with an indirect spin-flip band gap of 0.05 eV.

Impurity-band Stoner ferromagnetism has been proposed in hydrogen-chemisorbed graphene [19], CaB_6 [30], and even in the diluted ferromagnetic semiconductors [31], where the impurity bands are superposed on the underlying metallic band structure [19,30,31]. The fcc C_{60} is a direct band gap semiconductor, and the chemisorbed hydrogen creates a single impurity band within the band gap, resulting in a much simpler and verifiable electronic structure. In impurity-band Stoner ferromagnetism, the Curie temperature is of the order of the exchange splitting [30]. The exchange splitting of 0.2 eV in the fcc $C_{60}H$ is large enough for room-temperature ferromagnetism. The magnetic moment per fcc $C_{60}H_n$ is 0.9 μ_B for $n = 1$ or 5 and 0.8 μ_B for $n = 3$. In the fcc $C_{60}H_3$, the impurity-band width (~ 0.26 eV) increases, and thus the spin-split bands slightly overlap for a compensation of the spin density in the two spin-split bands. In the fcc $C_{60}H_5$, the exchange splitting (~ 0.26 eV) further increases to separate the spin-split bands, again leading to a ferromagnetic semiconductor with the same magnetic moments as that in the fcc $C_{60}H$. The 2D hexagonal polymer of $C_{60}H$ also showed Stoner ferromagnetism with the magnetic moment ~0.82 μ_B per $C_{60}H$ and the exchange splitting ~0.24 eV.

Each carbon atom of C_{60} has two 5:6 bonds and a 6:6 bond. The 5:6 bond is a σ bond of the sp^2 orbital lying between a pentagon and a hexagon. The 6:6 bond lying between two hexagons is a double bond comprising a σ

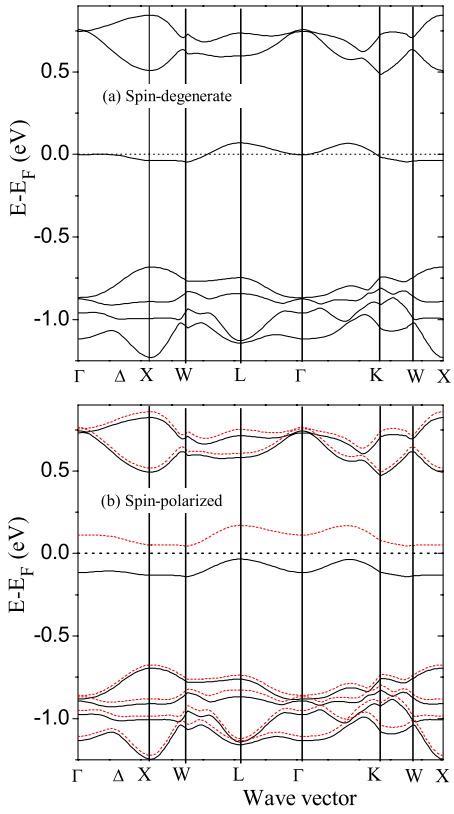

FIG. 3 (color online). Spin-degenerate (a) and spin-polarized (b) electronic structures of a fcc $C_{60}H$ crystal along the symmetry line in the fcc Brillouin zone. The dotted (red) and the solid (black) lines in (b) correspond to the spin-up and -down bands, respectively.

bond of the sp^2 orbital and a π bond. Chemisorbed hydrogen is bonded to a carbon atom with two 5:6 bonds (H5:6 bond) and a 6:6 bond (H6:6 bond). The hydrogen-chemisorbed carbon atom has sp^3-like bonds with bond angles of 111.4° and 110.8°, respectively, for C-C-C and H-C-C, the closed shell avoiding an additional electron occupation. A simple picture can thus be described as follows.

A H6:6 bond turns into a single σ bond of the sp^3 orbital breaking the π bond, one of the two π electrons taking part in the σ bond of the sp^3 orbital of the hydrogen-chemisorbed carbon atom and the other being quasilocalized around the opposite-side carbon atom on the H6:6 bond (delocalized over a fullerene surface centered at the H6:6 carbon atom). The quasilocalized π electrons create a spin-split state at the Fermi level giving a magnetic moment [Figs. 1(a) and 2(a)]. In the fcc $C_{60}H$, the quasilocalized π electrons overlap to produce a narrow half filled metallic band within the band gap, and the Stoner type of exchange interaction between the itinerant electrons renders the impurity band spin-split, leading to a ferromagnetic semiconductor. In the case of $C_{60}H_2$, the second hydrogen may take a number of configurations. The most stable configuration comprises two hydrogens bonded to the opposite sides of a 6:6 bond (H6:6H bond) [32,33], both of the π electrons taking part in the sp^3 orbital and giving rise to no quasilocalized states and no magnetic moments [Figs. 1(b) and 2(b)]. The fcc $C_{60}H_2$ is a direct band gap nonmagnetic semiconductor as is the fcc C_{60}.

In $C_{60}H_3$, the stable configuration comprises two hydrogens on the H6:6H bond, and the remaining hydrogen can take an arbitrary position forming a H6:6 bond. The position of the remaining hydrogen may slightly affect the stability and the electronic structure, but the magnetic and electronic properties are essentially unchanged (several, not all, configurations were checked). The two hydrogens on the H6:6H bond give rise to no quasilocalized states and no magnetic moment as in the case of $C_{60}H_2$, and the remaining hydrogen on the H6:6 bond gives rise to a quasilocalized state and a magnetic moment as in the case of $C_{60}H$. Indeed, the electronic structure of $C_{60}H_3$ is quite close to a sum of those of $C_{60}H$ and $C_{60}H_2$ [see Fig. 1(c)]. Further hydrogen doping in their stable form can be taken to produce a number of H6:6H bonds and only one H6:6 bond, at least for low doping concentrations (the $C_{60}H_n$ were checked up to $n = 5$). The magnetic moment of $C_{60}H_n$, thus, should always be equal to 1 μ_B per molecule for n odd or 0 for n even (including zero). Assuming that the second Lieb theorem for a bipartite lattice with a half filled band can be applied to fullerenes [19,34], the two hydrogens on the H6:6H bond can be considered to occupy opposite sublattices giving a zero magnetic moment.

$(C_{60}H)_2$, the dimer of $C_{60}H$, has a spin-triplet ground state with a magnetic moment of 1 μ_B per $C_{60}H$ [22]. The electronic structure of $(C_{60}H)_2$ in Fig. 1(e) shows an increase in the number of spin-split states near E_F, indicating that polymerization of $C_{60}H_n$ increases the density of states near E_F, resulting in a half filled impurity band just as in the fcc $C_{60}H_n$. The LDOS near E_F in Fig. 2(e) shows that the electrons of the spin-split states are quasilocalized in each $C_{60}H$ in the same way as in the monomers. The quasilocalized electrons in each $C_{60}H$ overlap to increase the spin-split states in $(C_{60}H)_2$, the LDOS on the bridging bond nearly vanishing [22].

The ground state of $(C_{60}H)_2$ is known to have mirror or inversion symmetry in the triplet spin state [22]. The $(C_{60}H)_2$ in Fig. 2(e) without such a symmetry depicts a minimal part of the 2D hexagonal polymer in order to show how the 2D hexagonal polymer of $C_{60}H$ leads to Stoner ferromagnetism. Considering symmetry, $C_{60}H_n$ crystal or polymer may have many distinct structures. The 2D hexagonal polymer as a 2D analogue to the 3D rhombohedral polymer has recently been an issue [21]. While the fcc structure of $C_{60}H_n$ with small n may not be the most stable form, in this work the fcc form of $C_{60}H_n$ was investigated in order to understand how the fcc $C_{60}H_n$ in general can attain ferromagnetism [25]. It is to be noted that a LDA calculation often underestimates the band gap, which can be compensated for by the generalized gradients

approximation. Our generalized gradients approximation calculation for fcc $C_{60}H$ implementing the Becke gradient exchange functional [35,36] yielded Stoner ferromagnetism as well, with an exchange splitting of ~0.37 eV well exceeding 0.2 eV as obtained by the LDA calculation, however, essential features of the band structure being preserved. In effect, hydrogen chemisorption in $C_{60}H_n$ with n odd creates a quasilocalized π electron, and a direct overlap of the π electrons leading to a half filled impurity band is essential for Stoner ferromagnetism while spin alternation, polymerization, and crystallization can only help with the overlap.

This work was supported by the National Research Foundation of Korea (NRL Program No. R0A-2008-000-20066-0).

*rscel@korea.ac.kr

[1] T. L. Makarova, B. Sundqvist, R. Höhne, P. Esquinazi, Y. Kopelevich, P. Scharff, V. A. Davydov, L. S. Kashevarova, and A. V. Rakhmanina, Nature (London) **413**, 716 (2001).
[2] V. N. Narozhnyi, K.-H. Müller, D. Eckert, A. Teresiak, L. Dunsch, V. A. Davydov, L. S. Kashevarova, and A. V. Rakhmanina, Physica (Amsterdam) **329B**, 1217 (2003).
[3] R. A. Wood, M. H. Lewis, M. R. Lees, S. M. Bennington, M. G. Cain, and N. Kitamura, J. Phys. Condens. Matter **14**, L385 (2002).
[4] T. L. Makarova and I. B. Zakharova, Fuller. Nanotub. Carbon Nanostructures **16**, 567 (2008).
[5] S. Okada and A. Oshiyama, Phys. Rev. B **68**, 235402 (2003).
[6] D. W. Boukhvalov, P. F. Karimov, E. Z. Kurmaev, T. Hamilton, A. Moewes, L. D. Finkelstein, M. I. Katsnelson, V. A. Davydov, A. V. Rakhmanina, T. L. Makarova, Y. Kopelevich, S. Chiuzbăian, and M. Neumann, Phys. Rev. B **69**, 115425 (2004).
[7] A. Talyzin, A. Dzwilewski, L. Dubrovinsky, A. Setzer, and P. Esquinazi, Eur. Phys. J. B **55**, 57 (2007).
[8] D. W. Boukhvalov and M. I. Katsnelson, Eur. Phys. J. B **68**, 529 (2009).
[9] T. L. Makarova, B. Sundqvist, R. Höhne, P. Esquinazi, Y. Kopelevich, P. Scharff, V. Davydov, L. S. Kashevarova, and A. V. Rakhmanina, Nature (London) **440**, 707 (2006).
[10] T. L. Makarova, K.-H. Han, P. Esquinazi, R. R. da Silva, Y. Kopelevich, I. B. Zakharova, and B. Sundqvist, Carbon **41**, 1575 (2003).
[11] F. J. Owens, Z. Iqbal, L. Belova, and K. V. Rao, Phys. Rev. B **69**, 033403 (2004).
[12] Y. Murakami and H. Suematsu, Pure Appl. Chem. **68**, 1463 (1996).
[13] J. A. Chan, B. Montanari, W. L. Chan, and N. M. Harrison, Mol. Phys. **103**, 2573 (2005).
[14] O. E. Kvyatkovskii and I. B. Zakharova, Fuller. Nanotub. Carbon Nanostructures **16**, 574 (2008).
[15] P. Esquinazi, D. Spemann, R. Hohne, A. Setzer, K-H. Han, and T. Butz, Phys. Rev. Lett. **91**, 227201 (2003).
[16] K. W. Lee and C. E. Lee, Phys. Rev. Lett. **97**, 137206 (2006); K. W. Lee, H. Kweon, J. J. Kweon, and C. E. Lee, J. Appl. Phys. **107**, 044302 (2010).
[17] A. L. Friedman, H. Chun, Y. J. Jung, D. Heiman, E. R. Glaser, and L. Menon, Phys. Rev. B **81**, 115461 (2010).
[18] C. H. Park and D. J. Chadi, Phys. Rev. Lett. **94**, 127204 (2005).
[19] O. V. Yazyev and L. Helm, Phys. Rev. B **75**, 125408 (2007).
[20] L. Pisani, B. Montanari, and N. M. Harrison, New J. Phys. **10**, 033002 (2008).
[21] J. A. Chan, B. Montanari, J. D. Gale, S. M. Bennington, J. W. Taylor, and N. M. Harrison, Phys. Rev. B **70**, 041403 (2004).
[22] O. E. Kvyatkovskii, I. B. Zakharova, A. L. Shelankov, and T. L. Makarova, Phys. Rev. B **72**, 214426 (2005).
[23] G. B. Allemand, K. C. Khrmani, A. Koch, F. Wudl, K. Holczer, S. Donovan, G. Gruner, and J. D. Thompson, Science **253**, 301 (1991).
[24] S. Garaj, T. Kambe, L. Forro, A. Sienkiewicz, M. Fujiwara, and K. Oshima, Phys. Rev. B **68**, 144430 (2003).
[25] V. E. Antonov, I. O. Bashkin, S. S. Khasanov, A. P. Moravsky, Y. G. Morozov, Y. M. Shulga, Y. A. Ossipyan, and E. G. Ponyatovsky, J. Alloys Compd. **330–332**, 365 (2002).
[26] S. Lobach, Yu. M. Shul'ga, O. S. Roshchupkina, A. I. Rebrov, A. A. Perov, Yu. G. Morozov, V. N. Spector, and A. A. Ovchinnikov, Fuller. Nanotub. Carbon Nanostructures **6**, 375 (1998).
[27] D. Sánchez-Portal, P. Ordejon, E. Artacho, and J. M. Soler, Int. J. Quantum Chem. **65**, 453 (1997); http://www.icmab.es/siesta/.
[28] V. Zólyomi, J. Koltai, J. Kürti, and S. Pekker, Phys. Status Solidi B **245**, 2018 (2008).
[29] N. Matsuzawa, D. A. Dixon, and P. J. Krusic, J. Phys. Chem. **96**, 8317 (1992).
[30] D. W. Edwards and M. I. Katsnelson, J. Phys. Condens. Matter **18**, 7209 (2006).
[31] J. M. D. Coey, P. Stamenov, R. D. Gunning, M. Venkatesan, and K. Paul, New J. Phys. **12**, 053025 (2010).
[32] N. Matsuzawa, D. A. Dixon, and T. Fukunaga, J. Phys. Chem. **96**, 7594 (1992).
[33] T. L. Makarova, I. B. Zakharova, O. E. Kvyatkovskii, S. G. Buga, A. P. Volkov, and A. L. Shelankov, Phys. Status Solidi B **246**, 2778 (2009).
[34] E. H. Lieb, Phys. Rev. Lett. **62**, 1201 (1989).
[35] A. D. Becke, Phys. Rev. A **38**, 3098 (1988).
[36] C. Lee, W. Yang, and R. G. Parr, Phys. Rev. B **37**, 785 (1988).